Proceedings of the Institution of Civil Engineers
**Water & Maritime Engineering 148**
September 2001 Issue 3
Pages 167–175

**Paper 12220**
Received 18/11/1999
Accepted 10/10/2000

**Keywords:**
hydraulics & hydrodynamics/ mathematical modelling/river engineering

**Clive G. Mingham**
Senior Lecturer, Department of Computing and Mathematics, Manchester Metropolitan University

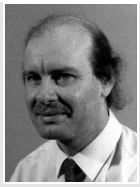

**Derek M. Causon**
Professor, Department of Computing and Mathematics, Manchester Metropolitan University

**David M. Ingram**
Senior Lecturer, Department of Computing and Mathematics, Manchester Metropolitan University

# A TVD MacCormack scheme for transcritical flow

C. G. Mingham, D. M. Causon and D. M. Ingram

**A simple update to a well-known classical scheme for solving the non-linear shallow water equations is described which is computationally efficient and able to resolve accurately both subcritical and supercritical flows. The solver is the MacCormack scheme with a total variation diminishing term appended to the corrector step which eliminates spurious numerical oscillations which often arise when the convective terms are discretized using classical central difference schemes. The scheme is explicit, second-order in space and time and formulated in finite volume form for ease of implementation on a general boundary conforming grid. Bench mark solutions in one and two dimensions involving both steady and non-steady flows are shown to illustrate the high spatial accuracy and computational efficiency of the method compared to the MacCormack schemes and a modern Riemann-based upwind scheme.**

## 1. INTRODUCTION

Numerical models based on the non-linear shallow water equations are being used increasingly by the hydraulic engineer as a cost-effective way to analyse a wide range of coastal and estuarine flow problems. Discontinuous solutions corresponding to transcritical flow features such as bores and hydraulic jumps may be caused by rapid variations in channel topography (e.g. estuarine narrowing, sand bars) or by wave diffraction and reflection (e.g. current deflecting walls, harbour entrances). These give rise to high spatial gradients in depth and velocity, the resolution of which presents a severe challenge to classical numerical schemes. Such schemes exhibit spurious oscillations around flow discontinuities and require artificial viscosity terms to stabilise the solution. In many cases the schemes contain adjustable parameters which require calibration. Modern upwind schemes based on Riemann solvers avoid these problems and resolve high gradients accurately but at extra cost in computational time.[1–3] The authors present a total variation diminishing (TVD) version of a classical explicit second-order accurate scheme (the MacCormack scheme) which removes unwanted non-physical oscillations with little extra computational cost and without any adjustable parameters to calibrate.[4] The scheme is significantly easier to implement than other TVD variants of the MacCormack scheme and is formulated in finite volume form so that complex geometries can be represented accurately with a boundary conforming mesh.[5,6] In many cases, the results produced compare favourably with modern Riemann-based upwind schemes and are obtained at lower computational cost, thus allowing existing codes to be updated very effectively.

## 2. DEFINING EQUATIONS

The integral form of the two-dimensional shallow water equations (SWEs) taken over a planar region $A$ with boundary $S$ and outward pointing unit normal vector $\boldsymbol{n}$ are

$$\frac{\partial}{\partial t}\iint_A \boldsymbol{U}dA + \oint_S \boldsymbol{H}\cdot\boldsymbol{n}dS = \iint_A \boldsymbol{Q}dA + \oint_S \boldsymbol{H}_v\cdot\boldsymbol{n}dS \quad (1)$$

where

$$\boldsymbol{Q} = \boldsymbol{A} + \boldsymbol{B} + \boldsymbol{C} + \boldsymbol{D}$$

$$\boldsymbol{A} = \begin{bmatrix} 0 \\ fv\phi \\ -fu\phi \end{bmatrix}, \quad \boldsymbol{B} = \begin{bmatrix} 0 \\ \left(\frac{g}{\rho}\right)\tau_{xw} \\ \left(\frac{g}{\rho}\right)\tau_{yw} \end{bmatrix}, \quad \boldsymbol{C} = \begin{bmatrix} 0 \\ -\left(\frac{g}{\rho}\right)\tau_{xf} \\ -\left(\frac{g}{\rho}\right)\tau_{yf} \end{bmatrix},$$

$$\boldsymbol{D} = \begin{bmatrix} 0 \\ \phi g b_x \\ \phi g b_y \end{bmatrix}$$

$$\boldsymbol{U} = \begin{bmatrix} \phi \\ \phi u \\ \phi v \end{bmatrix}, \quad \boldsymbol{H} = \begin{bmatrix} \phi\boldsymbol{q} \\ \phi u\boldsymbol{q} + 0{\cdot}5\phi^2\boldsymbol{i} \\ \phi v\boldsymbol{q} + 0{\cdot}5\phi^2\boldsymbol{j} \end{bmatrix},$$

$$H_v = \begin{bmatrix} 0 \\ \left(\frac{\phi}{\rho}\right)\sigma_{xx}\boldsymbol{i} + \left(\frac{\phi}{\rho}\right)\tau_{xy}\boldsymbol{j} \\ \left(\frac{\phi}{\rho}\right)\tau_{yx}\boldsymbol{i} + \left(\frac{\phi}{\rho}\right)\sigma_{yy}\boldsymbol{j} \end{bmatrix}$$

and $\phi = gh$ is the geopotential; $g$ is the acceleration due to gravity; $h$ is the water depth; $\boldsymbol{q} = u\boldsymbol{i} + v\boldsymbol{j}$ is the water velocity; $f$ is the coriolis force; $\rho$ is the water density; $\tau_{xw}$, $\tau_{yw}$ are wind shear stresses; $\tau_{xf}$, $\tau_{yf}$ are bed shear stresses; $\sigma_{xx}$, $\sigma_{yy}$, $\tau_{xy}$, $\tau_{yx}$ are the normal and shear stresses respectively; and $b_x$, $b_y$ are the bed slopes (measured downwards). $\boldsymbol{U}$ is the vector of conserved quantities and $\boldsymbol{H}$ and $\boldsymbol{H}_v$ are the inviscid convective and viscous flux terms respectively.

Here we concentrate on the convective terms which cause the most difficulty numerically. They are,

$$\frac{\partial}{\partial t}\iint_A \boldsymbol{U}dA + \oint_S H\cdot\boldsymbol{n}dS = 0 \quad (2)$$

Setting the right-hand side of equation (1) to zero removes all the source terms from the equation set so that the numerical results presented later are for model problems. Of course, for realistic engineering problems, source terms such as bed slope and friction are required on the right-hand side of equation (2). Details of how these terms are discretised in a finite volume setting are given in Reference 7.

## 3. FINITE VOLUME METHOD (FVM)

A finite volume form implementation of the numerical scheme is desirable so that the calculations can be carried out on a computational mesh which conforms to the complex boundaries encountered in practice. The physical region over which the equations are to be solved is tessellated by a structured mesh (indexed by $i, j$) of quadrilateral cells of area $A_{ij}$. $\boldsymbol{U}_{ij}$ is the integral average of $\boldsymbol{U}$ over cell $i,j$ located at the cell centre. Since equation (2) holds for an arbitrary region, it can be approximated over each cell as follows

$$\frac{\partial \boldsymbol{U}_{i,j}}{\partial t} = -\frac{1}{A_{i,j}} \sum_{k=1}^{4} \boldsymbol{H}_k \cdot \boldsymbol{S}_k \tag{3}$$

where the summation is taken over each side, $k$, of cell $i,j$ in turn and $\boldsymbol{S}_k$ is the outward pointing normal vector to side $k$ whose magnitude is the length of side $k$. $\boldsymbol{H}_k$ are the fluxes defined at the corresponding cell interfaces and based on neighbouring cell centre data.

## 4. TVD THEORY AND THE TVD MACCORMACK SCHEME

Schemes which are first-order accurate in space are formally monotone and do not introduce non-physical oscillations around bores and hydraulic jumps. However, they are much too dissipative for practical use, smearing the front over many mesh points, so it seems reasonable to use higher-order schemes. Godunov[8] showed that schemes of higher than first order cannot be monotone and will always produce spurious oscillations around discontinuities. This led to developments in so-called total variation diminishing (TVD) schemes which 'preserve monotonicity' by limiting oscillations through added non-linear artificial dissipation terms.[9] The theory was developed for the model one-dimensional scalar conservation, or solute transport equation and later extended to systems of equations such as equation (2).

### 4.1. TVD schemes for scalar equations

The one-dimensional scalar conservation equation in differential form with wave speed $v$ is

$$\frac{\partial u}{\partial t} + v\frac{\partial u}{\partial x} = 0 \tag{4}$$

Let $u_i^n$ be the numerical solution to equation (4) at $x = i\Delta x$, $t = n\Delta t$ where $\Delta x$, $\Delta t$ are the spatial and time steps respectively. The total variation of the solution is defined by

$$TV(u_i^n) = \sum_i |u_{i+1}^n - u_i^n| \tag{5}$$

A scheme is TVD if

$$TV(u_i^{n+1}) \leq TV(u_i^n) \tag{6}$$

Any three-point conservative finite difference scheme for solving equation (4) can be written in the so-called Harten[9] incremental form

$$u_i^{n+1} = u_i^n - A_{i-1/2}\Delta u_{i-1/2}^n + B_{i+1/2}\Delta u_{i+1/2}^n \tag{7a}$$

where

$$\Delta u_{i+1/2} = u_{i+1} - u_i, \quad \Delta u_{i-1/2} = u_i - u_{i-1} \tag{7b}$$

Different schemes result in different forms for the coefficients $A$ and $B$. It can be shown that a necessary and sufficient condition for such a scheme to be TVD is

$$A_{i+1/2} \geq 0, \quad B_{i+1/2} \geq 0, \quad 0 \leq A_{i+1/2} + B_{i+1/2} \leq 1 \tag{8}$$

Most classical schemes (e.g. the MacCormack scheme) are not TVD and do not satisfy the constraints (equation (8)).

Sweby[10] and later Davis[11] converted a non-TVD, and therefore oscillatory, scheme into a TVD scheme by modifying the coefficients $A$ and $B$ in order to satisfy equation (8). The starting point is the well-known Lax-Wendroff (L-W) scheme

$$u_i^{n+1} = u_i^n - \upsilon\Delta u_{i-1/2}^n - \nabla\left[\frac{1}{2}(1-\upsilon)\upsilon\Delta u_{i+1/2}^n\right]$$

where

$$\upsilon = v\frac{\Delta t}{\Delta x} \quad \text{and} \quad \nabla u_i^n = u_i^n - u_{i-1}^n$$

which can be written as the first-order scheme

$$u_i^{n+1} = u_i^n - \upsilon\Delta u_{i-1/2}^n \tag{9a}$$

with an additional anti-diffusive flux term

$$-\nabla\left[\frac{1}{2}(1-\upsilon)\upsilon\Delta u_{i+1/2}^n\right] \tag{9b}$$

Since equation (9a) is known to be monotone (because it is first-order) we proceed by adding only a limited amount of the second-order anti-diffusive flux (equation (9b)) to give

$$u_i^{n+1} = u_i^n - \upsilon\Delta u_{i-1/2}^n - \nabla\left[\phi\frac{1}{2}(1-\upsilon)\upsilon\Delta u_{i+1/2}^n\right] \tag{10}$$

where $\phi$ is a flux limiter function.

Equation (10) can then be written in the form

$$u_i^{n+1} = u_i^n - \upsilon\left\{1 + \frac{1}{2}(1-\upsilon)\left[\frac{\phi(r_i^+)}{r_i^+} - \phi(r_{i-1}^+)\right]\right\}\Delta u_{i-1/2}^n \tag{11}$$

where

$$r_i^+ = \frac{\Delta u_{i-1/2}^n}{\Delta u_{i+1/2}^n} \tag{12}$$

is known as a ratio of successive gradients.

So constructed, equation (11) reproduces the L-W scheme if

$\phi(r) = 1$. By comparing equation (11) with the incremental form of equation (7a), it is found that

$$A_{i-1/2} = v\left\{1 + \frac{1}{2}(1-v)\left[\frac{\phi(r_i^+)}{r_i^+} - \phi(r_{i-1}^+)\right]\right\} \quad (13a)$$

$$B_{i+1/2} = 0 \quad (13b)$$

and if we impose the constraints of equation (8) on $A$, $B$ we find that for the scheme of equation (11) to be TVD, the flux limiter function $\phi(r)$ must satisfy

$$0 \leq \left[\frac{\phi(r)}{r}, \phi(r)\right] \leq 2 \quad (14)$$

with the additional CFL stability condition

$$|v| \leq 1$$

That is, the flux limiter must lie within the hatched region of Fig 1(a).

It can be further shown that the hatched region illustrated in Fig. 1(b) corresponds to the second-order TVD region.

Since it is known that the unmodified L-W scheme is not TVD, and that the L-W coefficients do not satisfy the constraints of equation (8), we can devise appropriate corrective terms to amend the coefficients such that they do satisfy equation (8). Suitable terms are

$$G(r_i^+)\Delta u_{i+1/2}^n - G(r_{i-1}^+)\Delta u_{i-1/2}^n \quad (15)$$

where

$$G(r_i^+) = \frac{v}{2}(1-v)[1 - \phi(r_i^+)] \quad (16)$$

and $\phi$ satisfies equation (14). However, equation (15) is upwind weighted and therefore the precise form of equation (16) changes as the sign of the wavespeed $v$ in equation (4) changes. This unwanted complication can be removed to produce a five-point, symmetric, L-W TVD scheme by replacing equation (16) by

$$[G(r_i^+) + G(r_{i+1}^-)]\Delta u_{i+1/2}^n - [G(r_{i-1}^+) + G(r_i^-)]\Delta u_{i-1/2}^n \quad (17)$$

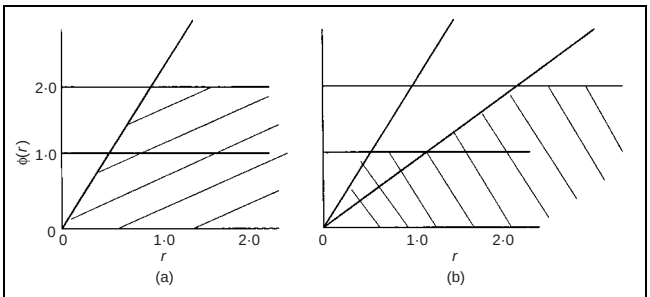


Fig. 1. Diagrams showing: (a) flux limiter functions; and (b) TVD regions

where

$$r_i^- = \frac{\Delta u_{i+1/2}^n}{\Delta u_{i-1/2}^n} \quad (18)$$

$$G(r_i^\pm) = \frac{|v|}{2}(1-|v|)[1 - \phi(r_i^\pm)] \quad (19)$$

These results can be extended easily to scalar non-linear problems by defining a local Courant number to replace the global definition

$$v = v\frac{\Delta t}{\Delta x}$$

### 4.2. Extension to the coupled SWE

In order to extend this scalar scheme to the coupled SWE, it is first necessary to consider the constant coefficient system

$$\frac{\partial \boldsymbol{U}}{\partial t} + A\frac{\partial \boldsymbol{U}}{\partial x} = \boldsymbol{0} \quad (20)$$

where $\boldsymbol{U}$ is the solution vector defined in equation (1) and $A$ is a $3 \times 3$ constant Jacobian matrix. If $P$ denotes the matrix which diagonalises $A$, then

$$P^{-1}AP = D = \text{diag}\ (\lambda_m) \quad (21)$$

where $\lambda_m$ are the eigenvalues of $A$.

We proceed by uncoupling equation (20) by defining new dependent variables

$$\boldsymbol{V} = P^{-1}\boldsymbol{U} \quad (22)$$

then, multiplying equation (20) by $P^{-1}$, yields

$$P^{-1}\boldsymbol{U}_t + P^{-1}A\boldsymbol{U}_x = \boldsymbol{0} \quad (23)$$

which is

$$\boldsymbol{V}_t + D\boldsymbol{V}_x = \boldsymbol{0} \quad (24)$$

which is the uncoupled form of the SWE.

In principle, equation (24) can be solved by applying the TVD L-W scheme to each scalar equation in turn, that is

$$\begin{aligned}\boldsymbol{V}_i^{n+1} = {} & \boldsymbol{V}_i^n - \frac{v}{2}[\boldsymbol{V}_i^n - \boldsymbol{V}_{i-1}^n] + \frac{v^2}{2}[\boldsymbol{V}_{i+1}^n - 2\boldsymbol{V}_1^n + \boldsymbol{V}_{i-1}^n] \\ & + [G(r_i^+) + G(r_{i+1}^-)]\Delta\boldsymbol{V}_{i+1/2}^n - [G(r_{i-1}^+) + G(r_i^-)]\Delta\boldsymbol{V}_{i-1/2}^n\end{aligned} \quad (25)$$

However, to obtain a numerical scheme in terms of the original dependent variables, we multiply by $P^{-1}$. The result is

$$\begin{aligned}\boldsymbol{U}_i^{n+1} = {} & \boldsymbol{U}_i^n - A\frac{\Delta t}{2\Delta x}[\boldsymbol{U}_{i+1}^n - \boldsymbol{U}_{i-1}^n] \\ & + A^2\frac{\Delta t^2}{2\Delta x^2}[\boldsymbol{U}_{i+1}^n - 2\boldsymbol{U}_1^n + \boldsymbol{U}_{i-1}^n] + P[G(r_i^+) \\ & + G(r_{i+1}^-)]P^{-1}\Delta\boldsymbol{U}_{i+1/2}^n - P[G(r_{i-1}^+) + G(r_i^-)]P^{-1}\Delta\boldsymbol{U}_{i-1/2}^n\end{aligned} \quad (26)$$

which requires that we compute matrices $P$ and $P^{-1}$. This restriction can be removed, leading to a simpler formulation

than other available TVD L-W-type schemes by approximating the diagonal matrices $G$ by $G$ bar where

$$\bar{G}(r^{\pm}) = G(r^{\pm})I \tag{27}$$

where $I$ is the $3 \times 3$ identity matrix and

$$r_i^{+} = \frac{\langle \Delta \boldsymbol{U}_{i-1/2}^n, \Delta \boldsymbol{U}_{i+1/2}^n \rangle}{\langle \Delta \boldsymbol{U}_{i+1/2}^n, \Delta \boldsymbol{U}_{i+1/2}^n \rangle} \tag{28a}$$

$$r_i^{-} = \frac{\langle \Delta \boldsymbol{U}_{i-1/2}^n, \Delta \boldsymbol{U}_{i+1/2}^n \rangle}{\langle \Delta \boldsymbol{U}_{i-1/2}^n, \Delta \boldsymbol{U}_{i-1/2}^n \rangle} \tag{28b}$$

where $\langle , \rangle$ indicates the usual scalar product.[5,6]

With these approximations, the TVD L-W scheme for the coupled SWE takes the form

$$\begin{aligned} \boldsymbol{U}_i^{n+1} = \boldsymbol{U}_i^n &- A\frac{\Delta t}{2\Delta x}[\boldsymbol{U}_{i+1}^n - \boldsymbol{U}_{i-1}^n] \\ &+ A^2\frac{\Delta t^2}{2\Delta x^2}[\boldsymbol{U}_{i+1}^n - 2\boldsymbol{U}_1^n + \boldsymbol{U}_{i-1}^n] + [\bar{G}(r_i^{+}) \\ &+ \bar{G}(r_{i+1}^{-})]\Delta \boldsymbol{U}_{i+1/2}^n - [\bar{G}(r_{i-1}^{+}) + \bar{G}(r_{i+1}^{-})]\Delta \boldsymbol{U}_{i-1/2}^n \end{aligned} \tag{29}$$

In these applications, the first three terms of equation (29) are replaced by the finite volume version of the well-known MacCormack scheme. This scheme is equivalent to the L-W scheme for scalar problems. While there is no guarantee that the TVD property will be preserved when scalar TVD schemes are extended to the systems case, numerical experience suggests that the schemes are largely non-oscillatory.

In the following section, the L-W scheme (equation (29)) will be replaced by the finite volume TVD MacCormack scheme for equation (2) in one dimension. Equation (2) may be solved on a two-dimensional structured mesh by applying a sequence of one-dimensional schemes via Strang operator splitting.[12] The MacCormack scheme is a two-stage predictor-corrector scheme defined as follows

(*a*) Predictor:

$$\boldsymbol{U}_i^{\overline{n+1}} = \boldsymbol{U}_i^n - \frac{\Delta t}{A_i}(\boldsymbol{H}_i^n \cdot \boldsymbol{S}_{i+1/2} + \boldsymbol{H}_{i-1}^n \cdot \boldsymbol{S}_{i-1/2}) \tag{30a}$$

(*b*) Corrector:

$$\boldsymbol{U}_i^{n+1} = 0{\cdot}5\left[\boldsymbol{U}_i^n + \boldsymbol{U}_i^{\overline{n+1}} - \frac{\Delta t}{A_i}(\boldsymbol{H}_{i+1}^{\overline{n+1}} \cdot \boldsymbol{S}_{i+1/2} + \boldsymbol{H}_i^{\overline{n+1}} \cdot \boldsymbol{S}_{i-1/2})\right] \tag{30b}$$

### 4.3. A TVD MacCormack scheme for the SWE

Based on the previous analysis of the preceding section, a particularly simple prescription can be defined for the TVD MacCormack scheme for the SWE simply by adding a local correction term, $TVD_i$, to the *corrector* step (equation (30b)). The term $TVD_i$ is defined as follows

$$TVD_i = [G(r_i^{+}) + G(r_{i+1}^{-})]\Delta \boldsymbol{U}_{i+1/2}^n - [G(r_{i-1}^{+}) + G(r_i^{-})]\Delta \boldsymbol{U}_{i-1/2}^n \tag{31a}$$

where

$$\Delta \boldsymbol{U}_{i+1/2}^n = \boldsymbol{U}_{i+1}^n - \boldsymbol{U}_i^n, \quad \Delta \boldsymbol{U}_{i-1/2}^n = \boldsymbol{U}_i^n - \boldsymbol{U}_{i-1}^n \tag{31b}$$

$$G(r_i^{\pm}) = 0{\cdot}5C(\upsilon_i)[1 - \phi(r_i^{\pm})] \tag{31c}$$

where $\upsilon_i$ is the local Courant number defined as

$$\upsilon_i = \frac{A_i}{(|\boldsymbol{q}_i \cdot \boldsymbol{S}_{i+1/2}| + \sqrt{\phi}|\boldsymbol{S}_{i+1/2}|)} \tag{31d}$$

$$C(x) = \begin{cases} x(1-x), & x \le 0{\cdot}5 \\ 0{\cdot}25, & x > 0{\cdot}5 \end{cases} \tag{31e}$$

The flux limiter function is

$$\phi(x) = \begin{cases} \min(2x, 1), & x > 0 \\ 0, & x \le 0 \end{cases} \tag{31f}$$

and the ratio of gradients is defined by

$$r_i^{+} = \frac{\langle \Delta \boldsymbol{U}_{i-1/2}^n, \Delta \boldsymbol{U}_{i+1/2}^n \rangle}{\langle \Delta \boldsymbol{U}_{i+1/2}^n, \Delta \boldsymbol{U}_{i+1/2}^n \rangle}, r_i^{-} = \frac{\langle \Delta \boldsymbol{U}_{i-1/2}^n, \Delta \boldsymbol{U}_{i+1/2}^n \rangle}{\langle \Delta \boldsymbol{U}_{i-1/2}^n, \Delta \boldsymbol{U}_{i-1/2}^n \rangle} \tag{31g}$$

where the numerator and denominator in each case involve a scalar product over the components of gradients of the solution vector $\boldsymbol{U}$.

The allowable time step, $\Delta t$, is defined by the usual CFL condition as

$$\Delta t = \upsilon \min_i\{\upsilon_i\} \tag{32}$$

In these calculations, $\upsilon$ was taken as 0·9 to ensure stability.

The present TVD MacCormack scheme has two important advantages over similar so-called TVD MacCormack finite difference schemes presented recently.[5,6] The appended TVD term (equation (31a)) is derived in a much simpler form and is easier to calculate than the corresponding corrective terms in the other schemes which are cast in terms of right-eigenvectors and Roe's averages, and, because the scheme is formulated in finite volume rather than the alternate finite difference form, it can be implemented on a general boundary-conforming mesh.

## 5. NUMERICAL RESULTS AND DISCUSSION

This paper demonstrates the performance of the modified scheme by applying it to several non-steady and steady problems in transcritical and supercritical flow. The results are compared with those obtained with a modern Riemann-based upwind scheme. The Riemann-based scheme (RBS) used for comparison purposes has been discussed in detail previously by the authors.[1] Other similar RBSs can be found in Reference 3. Generally speaking, these schemes represent the best currently available for transcritical flow.

### 5.1. Test I: one-dimensional dam break

This one-dimensional problem presents a severe test of any numerical advection scheme because of the discontinuity in the water depth. A domain of length 1·0 m was discretized using 100 cells. Initially, the water was at rest with depth 1·0 m in the left half of the domain and 0·5 m in the right half. The test was run for 0·05 s and transmissive boundary conditions were used

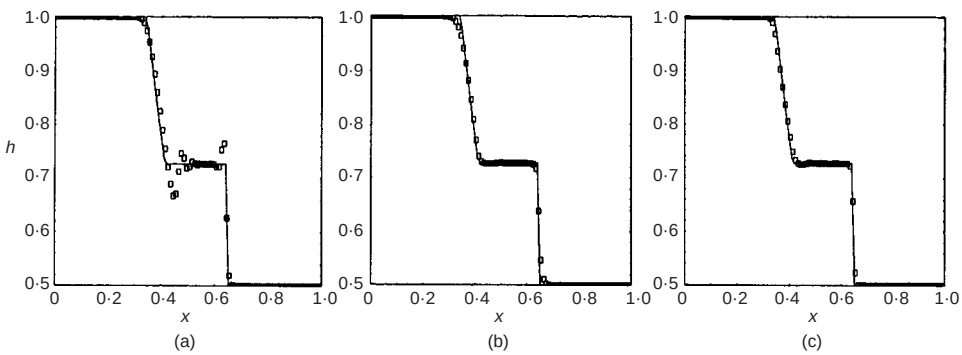


Fig. 2. Test 1—Comparison of numerical solution for water depth (squares) with exact solution for a one-dimensional dam break: (a) MAC; (b) MACTVD; and (c) Riemann-based scheme

at each end of the domain. Fig. 2 compares the exact solution for water depth to results obtained by the MacCormack scheme (MAC), MacCormack scheme with TVD correction (MACTVD) and a modern RBS.[1]

The exact solution consists of three regions of constant water depth separated by a right-travelling bore wave and a left-travelling depression wave. The MacCormack scheme oscillates wildly between the head of the depression and the start of the bore. As time progresses, these oscillations destroy the character of the solution and lead to non-physical (negative) water depths. In contrast, the MACTVD scheme is non-oscillatory and shows good agreement with the exact solution. In particular, the bore wave is resolved over only four cells. The Riemann-based scheme shows only a slight improvement in accuracy over the MACTVD scheme at the expense of a 40% increase in CPU time. Table 1 summarises the performance of the three schemes in terms of accuracy and speed. The following tests are even more stringent problems for which *no* stable solutions could be obtained with the unmodified MacCormack scheme; accordingly, it is discounted in the remaining comparisons of solutions.

**5.2. Test 2: steady supercritical flow in a converging channel**

This problem involves steady supercritical flow through a converging channel with its side walls inclined into the direction of flow. Such a flow scenario might arise in practice when flood water is conveyed along a spillway channel. The channel geometry is illustrated in Fig. 3(a). The water is assumed to enter the channel at a constant state with depth 1·0 m, zero transverse velocity and a Froude number of 2·7. This state was maintained at the left-hand (inflow) boundary throughout a time-marched calculation to a steady-state solution. Solid boundary conditions were used at the upper and lower channel walls and transmissive boundary conditions were used at the right-hand (outflow) boundary. The channel was symmetrical and defined by the wall deflection angle $\delta$, width $W$ and lengths $L1$, $L2$ and $L3$ (metres). A body fitted mesh was

| Test 1 | MAC | MACTVD | RBS |
|---|---|---|---|
| Relative CPU time | 1·00 | 1·49 | 2·10 |
| RMS error | 0·0154 | 0·0117 | 0·0098 |
| **Test 2** | **Exact** | **MACTVD** | **RBS** |
| Actual CPU time* | — | 4 h 2 min | 8 h 34 min |
| $\alpha$ | 33·69° | 34° | 34° |
| $\beta$ | 48·102° | 48° | 48° |
| $h_1$ | 1·00 | 1·00 | 1·00 |
| $h_2$ | 1·68 | 1·68 | 1·68 |
| $h_3$ | 2·561 | 2·562 | 2·562 |
| $Fr_1$ | 2·70 | 2·70 | 2·70 |
| $Fr_2$ | 1·8675 | 1·87 | 1·87 |
| $Fr_3$ | 1·2485 | 1·24 | 1·25 |
| **Test 3 CPU time** | | **MACTVD** | **RBS** |
| $t$ = 0·067 s | | 37 min 50 s | 63 min 5 s |
| $t$ = 0·125 s | | 55 min 54 s | 1 h 35 min 28 s |
| $t$ = 0·21 s | | 1 h 44 min 35 s | 3 h 1 min 30 s |
| $t$ = 0·45 s | | 3 h 42 min 49 s | 6 h 31 min 29 s |

*Computations were performed on a silicon graphics 75 MHz power challenge L-series machine using version 7.0 of the Fortran 77 compiler.

*Notes*:
Test 1: numerical and exact solutions for the one-dimensional dam break.
Test 2: numerical and exact solutions for the two-dimensional converging channel.
Test 3: numerical solutions for the two-dimensional contraction–expansion channel.

Table 1. Comparison of speed* and accuracy of numerical schemes

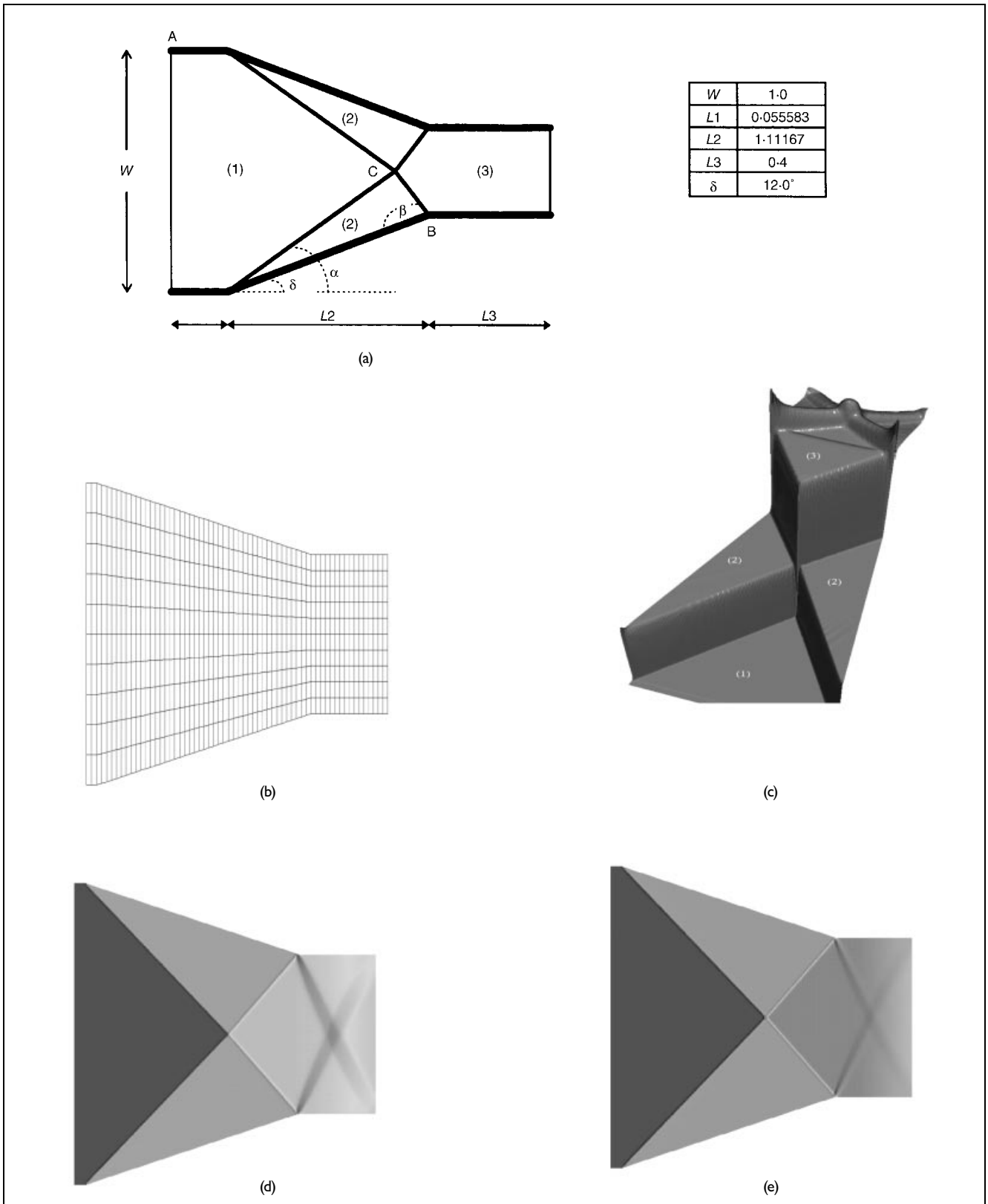


| | |
|---|---|
| $W$ | 1·0 |
| $L1$ | 0·055583 |
| $L2$ | 1·11167 |
| $L3$ | 0·4 |
| $\delta$ | 12·0° |

Fig. 3. Test 2—Steady-state supercritical flow in a converging channel: (a) geometry and regions of constant state; (b) schematic of computational mesh; (c) computer visualisation of water surface for MACTVD; (d) shaded water depth contours for MACTVD scheme; and (e) shaded water depth contours for Riemann-based scheme

constructed by dividing segments $L1$, $L2$ and $L3$ into 8, 160 and 56 equal intervals respectively. This produced a mesh with approximately uniform spacing in the $x$ direction. In the $y$ direction, 280 uniformly spaced cells were used. Fig. 3(b) shows the mesh layout. For clarity, the mesh illustrated is much coarser than the one actually used in the computations.

For this benchmark test problem, a steady-state solution can be calculated analytically.[13] At the start of the channel convergence, stationary oblique bore waves are formed inclined at $\alpha^\circ$ to each bank (see point A, Fig. 3(a)). The two bores are reflected at the centreline of the channel. By a suitable choice of channel geometry and left-hand inflow Froude number $(u(gh)^{-1/2})$, the

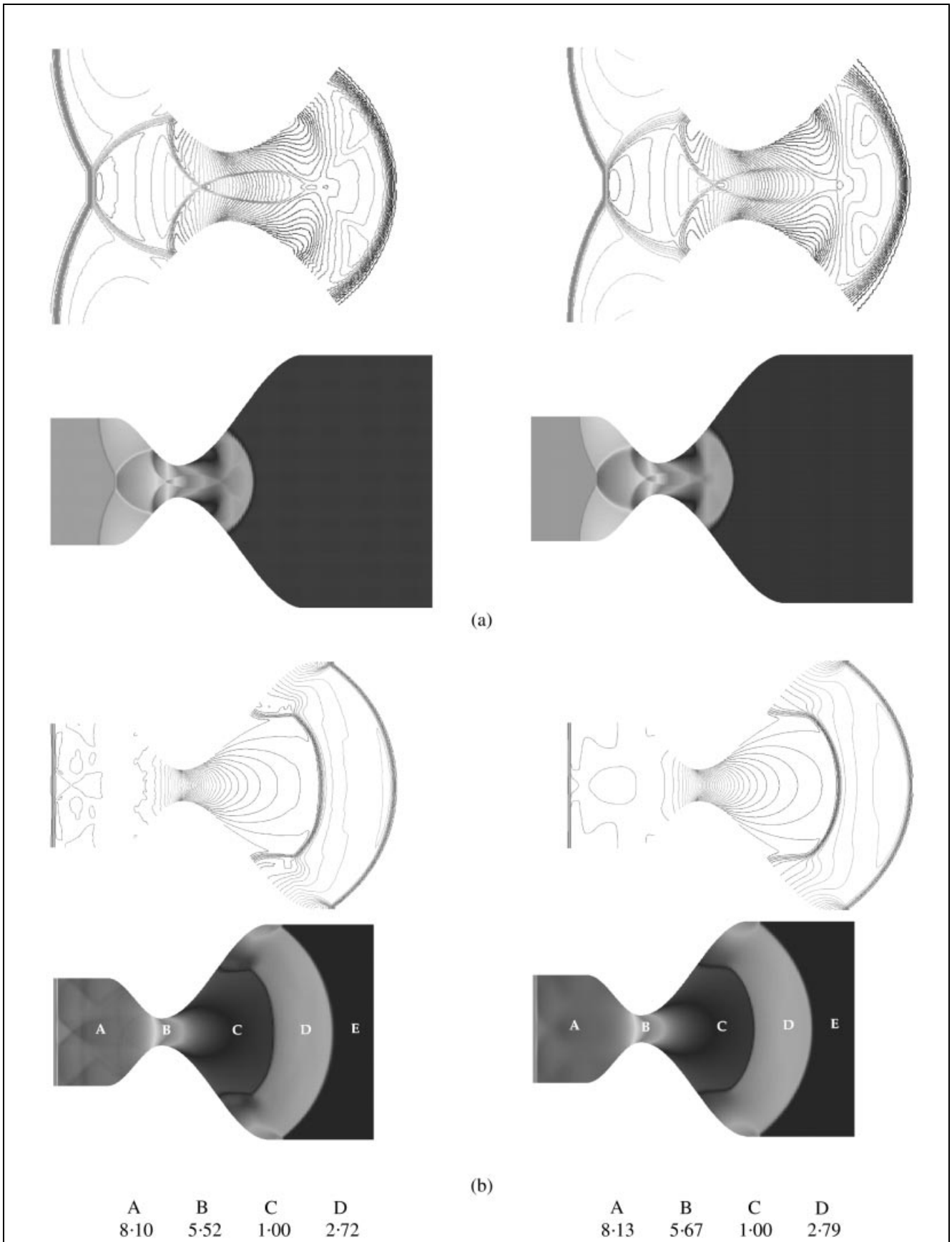


Fig. 4. Test 3—Comparision of water depth contours for bore diffraction in a contraction–expansion channel at time $t$ (s). Left column MACTVD, right column RBS: (a) $t = 0{\cdot}21$ s; and (b) $t = 0{\cdot}45$ s (line contours shown at expanded scales)

reflected waves can be arranged to meet the opposite bank at the point where the channel ceases its contraction (the necessary parameter settings in this case are given in Fig. 3(a)). In theory, complete wave cancellation can be expected at the end of the channel contraction (see point B, Fig. 3(a)). The net result is a partitioning of the converging channel into three distinct flow regions (1), (2) and (3) each of which is at a known constant state. The MACTVD scheme was run until the maximum relative error between current and previous water depths over the whole mesh was less than a prescribed tolerance, that is

$$\max_{i,j}\left(\frac{h_{i,j}^{n+1}-h_{i,j}^{n}}{h_{i,j}^{n}}\right) < tol$$

Normally, *tol* was set to $0{\cdot}5 \times 10^{-4}$. However, it was found that the solution with the MACTVD scheme had essentially converged with the residual oscillating around $5 \times 10^{-4}$, so the calculation was terminated after 2000 time steps. This behaviour is a well-known property of the MacCormack scheme. In the case of a Riemann-based scheme, the residual can normally be reduced by several orders of magnitude to the level of machine accuracy and the above setting for *tol* is appropriate. However, the precision achievable with the MACTVD scheme would be acceptable for most engineering purposes. Local time stepping, rather than a global minimum time step, was used in each case. Figs 3(c) and 3(d) show a visualisation of the water surface and shaded contour plot of depth respectively for the MACTVD scheme which show that this scheme reproduces the main features of the analytical solution without excessive numerical diffusion. Fig. 3(e) shows the results for the Riemann-based scheme which also required 2000 time steps.[1,13] Table 1 compares each scheme with the analytical solution (regions are denoted by subscripts). It can be seen that both schemes produce very accurate results but the MACTVD scheme is twice as fast as the Riemann-based scheme, saving 4 h of CPU time. In each case, almost complete wave cancellation occurs at the end of the contraction. Some evidence of a centred depression remains in both cases but this is an extremely weak feature and is due to the numerical dissipation inherent in each scheme. A number of other analytical benchmark test problems for steady supercritical flow have been given recently by the authors.[13]

### 5.3. Test 3: unsteady bore diffraction in a contraction–expansion channel

This two-dimensional unsteady flow problem presents a severe test of numerical schemes as it includes the complex processes of Mach reflection at the channel walls and multiple bore-on-bore interactions. This problem relates to a bore wave travelling along a curved channel which may arise in practice in the case of tidal bore wave propagation.

A channel, symmetric about the $x$ axis in the $x$–$y$ plane, was defined by the equation of its upper bank as follows

$$y = \begin{cases} 1{\cdot}0, & -2 \le x \le -1 \\ -0{\cdot}375\cos(\pi x) + 0{\cdot}625, & -1 < x \le 0 \\ -0{\cdot}625\cos(0{\cdot}5\pi x) + 0{\cdot}875, & 0 < x \le 2 \\ 1{\cdot}5, & 2 < x \le 4 \end{cases}$$

A bore wave positioned parallel to the $y$ axis and initially located at $x = -1{\cdot}0$ propagates from left to right along the channel with bore Froude number $F_B = 3$. The initial undisturbed state of the water to the right of the bore was given by $h_R = 1{\cdot}0$ with zero velocity components, while the left-hand state was completely specified by $v_L = 0$ and $F_B$ according to

$$h_L = 0{\cdot}5h_R(-1+\sqrt{1+8F_B^2}), \quad u_L = F_B(1-h_Rh_L^{-1})\sqrt{gh_R}$$

A body fitted mesh (constructed in a similar way to that in test 2) was used with 300 cells in the $x$ direction and 200 cells in the $y$ direction. Results at times $t = 0{\cdot}21$ s (Fig. 4(a)) and $0{\cdot}45$ s (Fig. 4(b)) are shown as line and shaded contour plots of depth for both the MACTVD and corresponding RBS schemes.[1,14] These figures show complex bore-on-bore interactions and reflections as the incident bore wave passes down the channel. Although this problem does not have an analytical solution, the MACTVD scheme captures the expected flow features and resolves the associated high spatial gradients. The MACTVD results compare favourably with a grid independent solution obtained with the RBS scheme and with other modern high-resolution Riemann-based schemes.[2,14] Table 1 compares CPU times for the two schemes. For the two runs it was found that the MACTVD scheme was approximately 170% faster on average than the RBS scheme.

## 6. CONCLUSIONS

It has been shown that the MacCormack scheme may be easily converted into a total variation diminishing scheme by appending appropriate terms to the corrector step. By so doing, the new scheme can be used to solve problems involving high spatial gradients such as bore waves and hydraulic jumps which are areas where classical schemes have been found to perform badly (or fail to perform at all). Furthermore, when compared to a modern Riemann-based solver, the MACTVD scheme is considerably more efficient computationally, while being of sufficient accuracy for most hydraulic engineering problems. Formulation of the MACTVD scheme in finite volume form also permits the use of boundary-conforming meshes for maximum flexibility in practice. The examples shown and description of the TVD correction terms illustrate that in principle it would be possible to convert other existing solvers into TVD schemes and so extend their range of applicability without the considerable expense of rewriting software.

## REFERENCES


1. Mingham C. G. and Causon D. M. High resolution finite volume method for shallow water flows. *Journal of Hydraulic Engineering*, 1998, **124**, No. 6, 605–614.
2. Yang J. Y. and Hsu C. A. Computations of free-surface flows. *Journal of Hydraulic Research*, 1993, **31**, No. 3, 403–414.
3. Zhao D. H. *et al.* Approximate Riemann solvers in FVM for 2D hydraulic shock wave modelling. *Journal of Hydraulic Engineering*, 1996, **122**, No. 12, 692–702.
4. MacCormack R. W. *The Effect of Hypervelocity Impact Cratering.* 1969, AIAA paper No. 69-354.
5. Garcia-Navarro P., Alcrudo F. and Saviron J. M., 1D open-channel flow simulation using a TVD-MacCormack scheme. *Journal of Hydraulic Engineering*, 1992, **118**, No. 10, 1359–1371.
6. Alcrudo F., Garcia-Navarro P. and Saviron J. M. Flux

difference splitting for 1D open channel flow equations. *International Journal of Numerical Methods in Fluids*, 1992, **14**, 1009–1018.
7. HU K., MINGHAM C. G. and CAUSON D. M. A bore-capturing finite volume method for open-channel flows. *International Journal of Numerical Methods in Fluids*, 1998, **28**, 1241–1261.
8. GODUNOV S. K. A difference method for the numerical calculation of discontinuous solutions of hydrodynamic equations. *Mat. Sbornik*, 1959, **47**, No. 3, 271–306.
9. HARTEN A. High resolution schemes for hyperbolic conservation laws. *Journal of Computational Physics*, 1983, **49**, 357–392.
10. SWEBY P. K. High resolution schemes using flux limiters for hyperbolic conservation laws. *SIAM Journal of Numerical Analysis*, 1984, **21**, No. 5, 995–1011.
11. DAVIS S. F. A simplified TVD finite-difference scheme via artificial viscosity. *SIAM Journal on Scientific and Statistical Computing*, 1987, **8**, No. 1, 1–18.
12. STRANG G. On the construction and comparison of finite difference schemes. *SIAM Journal of Numerical Analysis*, 1968, **5**, No. 3, 506–517.
13. CAUSON D. M., MINGHAM C. G. and INGRAM D. M. Advances in calculation methods for supercritical flow in channels. *Journal of Hydraulic Engineering*, 1999, **125**, No. 10, 1039–1050.
14. MINGHAM C. G. and CAUSON D. M. Calculation of unsteady bore diffraction using a high resolution finite volume method. *Journal of Hydraulic Research*, 2000, **38**, 49–56.

Please email, fax or post your discussion contributions to the secretary: email: kathleen.hollow@ice.org.uk; fax: +44 (0)20 7799 1325; or post to Kathleen Hollow, Journals Department, Institution of Civil Engineers, 1–7 Great George Street, London SW1P 3AA.